핵자기 공명 단층 촬영에서의 자화율 강조 영상법

노용만, 문치웅*, 임태환*, 조장희
한국과학기술원 전기및 전자 공학과, * 아산 생명 과학 연구소, NMR 연구실

Susceptibility Contrast Enhancement Imaging in MRI

Y. M. Ro, C. W. Mun*, T. H. Lim* and Z. H. Cho
Dept. of Electrical Science, Korea Advanced Institute of Science and Technology , P.O. Box 150, Chongyangni, * Asan Institute for Life Sciences, NMR Lab., Seoul, Korea

ABSTRACT

In MRI, an image contrast can be developed as a result of the susceptibility effect if an object has paramagnetic substances. This is mainly due to the non-uniform phase distribution or linear gradient developed by the magnetic susceptibility within a voxel, which in turn reduces the signal intensity; e.g., spin phases are dephased and thereby cancel each other resulting in a reduced signal. In this paper, a new concept for manipulating the susceptibility effect through the use of tailored RF pulses is proposed. As potential applications of the method, two different types of tailored RF pulses are introduced: one for susceptibility artifact correction and the other for contrast enhancement. The latter, for example, can be applied to angiography utilizing the paramagnetic property of deoxygenated blood. Both a theoretical study of the method and experimental results are reported.

I. INTRODUCTION

In Magnetic Resonance Imaging (MRI), paramagnetic substances influence the magnetic susceptibility; therefore, samples of paramagnetic materials tend to produce the well-known susceptibility effect (1-4). The susceptibility effect is similar to other field inhomogeneities observed in NMR imaging, such as the main magnetic field inhomogeneity and the chemical shift effects, but it differs slightly; i.e., it produces field variations at the interfaces of materials with different susceptibilities (5). The field variation due to the local susceptibility, however, has an exceptional property, i.e., it is much more abrupt so that even spins within a voxel experience sufficiently different phases from each other (6, 7). This susceptibility effect is particularly dominant in gradient echo imaging and appears as a signal loss; i.e., the different precession frequencies of the spins within a voxel result in a cancellation of the intravoxel signals (8). Recently, several attempts have been made to enhance the image contrast by using this "signal loss phenomenon" due to the susceptibility effect (9-12). This susceptibility contrast in an image due to the signal loss in a voxel is well known and can partly be avoided by the selection of thin slices (5).

In this paper, we will discuss this susceptibility contrast as a phase distribution problem in the slice-thickness direction and an attempt will be made to modify the inherent phase distribution by specially tailored, externally applied selection RF pulses (13). When a tailored RF pulse is used, it produces a particular phase distribution in a voxel which either enhances or reduces the intravoxel signal intensity so that the contrast is manipulated; i.e., superimposition of a particularly shaped phase distribution produced by the tailored RF pulse on the original phase distribution due to the susceptibility will lead to the desired phase distribution. In this paper, two types of tailored RF pulses are proposed as examples: one is an RF pulse which corrects the susceptibility artifact by simply enhancing the signal loss due to the susceptibility and the other is an RF pulse which enhances the signal in a voxel that exhibits the paramagnetic susceptibility effect (such as venous blood) but at same time suppresses the signals from non-paramagnetic substances such as normal tissues (14). The latter is obviously intended for angiographic applications.

II. THEORY AND METHODS

1. The Relationship between the Signal Intensity and the Susceptibility Effect

As mentioned above, the signal intensity from a voxel around materials having different magnetic susceptibilities is reduced due to spin dephasing within the voxel. Let us first analyze the relationship between the intravoxel signal intensity and the extent of the phase distribution generated by the susceptibility effect. Consider a voxel whose spins are distributed according to the field variation due to the susceptibility effect and assume that the slice thickness (along

the z-direction) is relatively thin so that the fields induced around the different susceptibility compartments are linear. Then, the phases of the spins in the voxel will be distributed linearly. Under these circumstances, the phase distribution in the slice-thickness direction (z-direction) due to the susceptibility-induced field variation in gradient echo imaging will be

$$\theta_{sus}(z) = \gamma T_E G_{SUS} z$$
$$\text{or} \quad = P_{sus} z \qquad [1]$$

where γ is the gyromagnetic ratio, T_E is the echo time, G_{SUS} is the field gradient created by the susceptibility difference between the paramagnetic substance and the surrounding tissue, and z is the position in the selected slice. In Eq. [1], we have defined the phase gradient, P_{sus}, which is induced by the susceptibility effect, as

$$P_{sus} = \gamma T_E G_{sus} . \qquad [2]$$

This phase gradient is a quantitative measure of the susceptibility effect within a voxel.

In the case of gradient echo imaging where a conventional sinc-shaped pulse is used as a selection RF pulse, the phase distribution along the slice-selection direction within the voxel is determined solely by the susceptibility-induced field, i.e., a constant phase distribution for the normal tissue but a strong linear phase distribution for the voxel affected by the susceptibility effect. This is due to the fact that the conventional sinc-shaped RF pulse has a constant phase (see Fig. 1 (a)). Consequently, the spins affected by the susceptibility will be dephased, and the intravoxel signal will be attenuated. The intravoxel signal, S, as a function of the susceptibility-induced phase gradient can be written as

$$S = \left| \int_{-\infty}^{\infty} M \, \text{rect}\left(\frac{z}{z_o}\right) \exp(i P_{sus} z) \, dz \right| \qquad [3]$$

where M is the magnetization, z_o is the slice thickness, and rect (z/z_o) is the rectangular function with a width of z_o. In this case, we have assumed that the transverse (x, y) resolution is much smaller than the resolution in the slice-selection direction and is also normalized so that the signal from the voxel is simply the integration of the magnetizations within the selected slice thickness. By a Fourier transform, under the assumption that P_{sus} is a variable, Eq. [3] can be written as

$$S = M z_o \left| \text{sinc}\left(\frac{P_{sus}}{2\pi} z_o\right) \right| . \qquad [4]$$

According to Eq. [4], the intravoxel signal decreases with increasing phase gradient (P_{sus}); furthermore, there is no signal intensity at phase gradients of $\pm 2\pi N/z_o$ where N is an integer. This means that the image contrast due to the susceptibility effect can be quantified by Eq. [4]. Consequently, if gradient echo imaging is used, a region where the susceptibility effect is large will appear as a signal void or a dark area in the image because of this intravoxel signal attenuation effect (see Fig. 2 (a)). The signal loss due to the susceptibility effect, therefore, will produce an image contrast. For example, the interfaces between the blood vessels and the surrounding tissues will appear in the image as dark lines due to the strong local field gradients produced at these interfaces (8).

2. Manipulation of the Susceptibility Effect by Use of the Tailored RF Pulses

As discussed above, the phase distribution of the spins in a voxel, which affects the signal intensity, is affected not only by the susceptibility-induced field variation but also by an externally applied slice-selection RF pulse (13). In conventional NMR imaging, the slice-selection RF pulse is in the form of a sinc function which has no particular phase distribution within the selected rectangular slice, i.e., a constant phase distribution in the slice-selection direction. A normal sinc RF pulse, therefore, does not affect the phase distribution of intravoxel spins within the selected slice. However, if one applies a tailored RF pulse which produces a desired phase distribution, one can alter the susceptibility-induced phase distribution in the selected slice, thereby affecting the signal intensity. Consequently, the image contrast due to the susceptibility effect can be manipulated by using tailored RF pulses. In the following, we will describe two such tailored RF pulses and their applications.

If a tailored RF pulse is designed so that the phase distribution generated by the RF pulse, $\theta_{RF}(z)$, gives a total phase distribution of intravoxel spins $\theta_{total}(z) = \theta_{sus}(z) + \theta_{RF}(z)$, the signal from the voxel will appear as

$$S = \left| \int_{-\infty}^{\infty} M \, \text{rect}\left(\frac{z}{z_o}\right) \exp\left[i \theta_{total}(z) \right] dz \right| \qquad [5]$$

or

$$S = \left| \int_{-\infty}^{\infty} M \, \text{rect}\left(\frac{z}{z_o}\right) \exp\left[i \theta_{RF}(z)\right] \exp\left(i P_{sus} z \right) dz \right| . \qquad [6]$$

By invoking the Fourier transform, Eq. [6] can be expressed as

$$S = \left| 2\pi M \, \mathcal{F}^{-1}\left[\text{rect}\left(\frac{z}{z_o}\right) \exp\left[i \theta_{RF}(z)\right] \right] \right| \qquad [7]$$

where $\mathcal{F}^{-1}(\cdot)$ represents the 1-D inverse Fourier transform operator. By using the convolution theorem, Eq. [7] can be rewritten as

$$S = \left| 2\pi M z_o \, \mathrm{sinc}\left(\frac{P_{sus}}{2\pi} z_o\right) * \mathcal{F}^{-1}\left[\exp\left[i\,\theta_{RF}(z)\right] \right] \right| \quad [8]$$

where * represents the convolution operator. As implied in Eq. [8], the signal intensity with a tailored RF pulse is the convolution of two functions: namely, the same function as given in Eq. [4] and a function which is the Fourier transform of the phase term of the intravoxel signal generated by the tailored RF pulse. This result indicates that the signal intensity given as a function of the strength of the susceptibility-induced phase gradient can be manipulated by an externally applied tailored RF pulse which produces an appropriate total phase distribution; i.e., by altering the phase distribution within a voxel with a suitable form, the desired signal intensity can be obtained.

Now, we will consider two applications using tailored RF pulses and the susceptibility effect as discussed above. The first application is the correction of the well-known susceptibility artifact, and the second is an application to the angiography using the susceptibility effect induced by either internally created deoxygenated blood (venous blood) or blood externally contrasted by administration of a paramagnetic agent such as Gd-DTPA.

(a) A tailored RF pulse producing a quadratic phase distribution

First, let us consider the reduction of the susceptibility artifact normally seen in gradient echo imaging. If the RF pulse is suitably tailored such that it produces a quadratic phase distribution ($\theta_{RF}(z) = \alpha z^2$, see Fig. 1 (b)) along the slice-selection direction, it can be used to compensate the phase dispersion due to the susceptibility. When a tailored RF pulse producing a quadratic phase is applied, the total phase distribution in the voxel will be modified, and the resulting signal intensity will become

$$S = \left| 2\pi M z_o \, \mathrm{sinc}\left(\frac{P_{sus}}{2\pi} z_o\right) * \mathcal{F}^{-1}\left[\exp(i\,\alpha z^2)\right] \right|. \quad [9]$$

Equation [9] clearly indicates that the superimposition of a quadratic-phase RF pulse distribution on the selected slice will enhance the total signal intensity as shown in Fig. 2 (b), provided that the susceptibility-dependent field inhomogeneity follows a linear field gradient pattern. Moreover, the widened uniform region of the signal shown in Fig. 2 (b) indicates that the signal strength is relatively constant up to a relatively large value of the susceptibility-induced field gradient. The signal strength, however, is reduced to $M_o Z_o/2$.

(b) A tailored RF pulse producing a bi-linear saw-tooth-like phase distribution

In our second application, a tailored RF pulse is applied in order to image blood containing deoxyhemoglobin. Blood containing deoxyhemoglobin is more paramagnetic than the surrounding tissues and produces a susceptibility effect at the blood-tissue interfaces (14-17). To image the blood only, the signals from the normal tissues should be suppressed while the signals from the blood interfaces, where strong susceptibility-induced fields exist, should be enhanced. To accomplished this goal, an RF pulse is tailored such that the selected slice has a phase distribution similar to a bi-linear saw-tooth-like distribution so that the spin phases are distributed uniformly from 0 to 2π radians ($\theta_{RF}(z) = 4\pi|z|/z_o$) along the slice-selection direction. The corresponding signal intensity then becomes

$$S = \left| 2\pi M z_o \, \mathrm{sinc}\left(\frac{P_{sus}}{2\pi} z_o\right) * \mathcal{F}^{-1}\left[\exp\left(i\,\frac{4\pi|z|}{z_o}\right)\right] \right|. \quad [10]$$

Figure 1 (c) shows the tailored RF pulse designed for this purpose. Figure 2 (c) presents the result from a numerical solution of Eq. [10] which shows the relationship between the signal intensity and the strength of the susceptibility-induced phase gradient. As is shown, in normal tissue, i.e., in the case of $P_{sus} = 0$, no signal is produced; therefore, signal suppression is achieved in normal tissues. However, on the other hand, the signal intensity increases monotonically with increasing phase gradient, at least up to $\pm 4\pi/z_o$; i.e., the signal intensity increases as the susceptibility-induced phase gradient increases. Consequently, this tailored RF pulse can effectively be used to suppress the signals from normal tissues while enhancing the signals from the blood-tissue interfaces where the susceptibility effect exists due to the deoxygenated blood, more specifically the deoxyhemoglobin. This type of RF pulse is, therefore, ideally suited for angiographic applications, especially for venography. This technique, however, is not limited to venography and can be extended to other angiographic applications if one uses externally administered paramagnetic contrast agents such as Gd-DTPA (18).

III. COMPUTER SIMULATIONS

We have performed computer simulations to verify the usefulness of the method. First, we have considered an imaging plane of water, which is located 5 cm away from the center of an air sphere having a radius of 2 cm. In this case, the magnetic field distribution in the imaging plane can be calculated and is shown in Fig. 3 (a) (6). As is shown in the figure, the magnetic field in the imaging plane is not uniform; hence, for a finite slice thickness, the intravoxel spins will be dephased and the signal intensity will be reduced even though the signal intensity in this plane should be uniform. In this simulation, we have assumed that the voxel consists of three hundred spins and that within a selected slice, the magnetic

field varies due to the susceptibility effect. Then, the phases of the spins will be distributed according to the field inhomogeneity within the selected slice, and the intravoxel signal intensity will be the vector sum of the magnetizations of these spins. All simulations were performed for a slice thickness of 1 cm with an echo time of 20 msec.

Figure 3 (b) shows the signal loss phenomenon when the conventional RF pulse is applied, which is known to be a susceptibility artifact around the air sphere,. The image contrast obtained shows that the signal intensity is reduced around the air sphere while other regions with no susceptibility effect show a relatively high signal intensity. If a tailored RF pulse which produces a quadratic phase distribution within the selected slice is applied, the signal loss shown in Fig. 3 (b) due to the susceptibility effect around the air sphere is recovered as shown in Fig. 3 (c); i.e., the susceptibility-dependent signal loss in the image is compensated for. This matches quite well with the results in Fig. 2 (b) where the signal intensity is almost independent of the susceptibility effect up to a certain value of the susceptibility phase gradient. Finally, by applying a tailored RF pulse which produces a bi-linear saw-tooth-like phase distribution within a selected slice, the image contrast reverses as shown in Fig. 3 (d); i.e., the signal intensities arising from the regions which have no field gradient are suppressed while the signal intensities arising from the regions where the susceptibility effect exists are enhanced.

In summary, as is shown in Fig. 3, the susceptibility-dependent contrast in an image can be manipulated by use of a suitably tailored RF pulse which will produce a desired phase distribution within a selected slice.

IV. EXPERIMENTAL RESULTS AND DISCUSSIONS

Experiments have been performed using the KAIS 2.0 T whole-body NMR imaging system and 4.7 T animal system. First, human imagings were performed with the gradient echo sequence in order to demonstrate that a tailored RF pulse producing a quadratic phase distribution will compensate for the signal loss due to the susceptibility effect. The echo time was 15 msec and the slice thickness was 1 cm. The value "α" in Eq. [9], which is a parameter of the quadratic phase generated by the tailored RF pulse, was $\frac{4\pi}{z_n^2}$. A human head imaging near the nasal cavities was then performed with and without the tailored RF pulse. The image shown in Fig. 4 (a) was obtained for the area near the nasal cavities using the conventional sinc RF pulse. As is seen, a strong susceptibility artifact is seen near the nasal cavities. Figure 4 (b) is the image obtained by applying the tailored RF pulse to produce a quadratic phase distribution within the selected slice. In that image, the susceptibility artifact is significantly reduced, and some pars of the tissue previously lost due to the susceptibility-dependent signal voids near the nasal cavities (dark areas) are fully recovered.

As another application, an RF pulse was designed to suppress the signals from the normal tissues but to enhance the signals from regions with local field gradients due to the susceptibility effect (19). This pulse, which has potential for angiographic applications, produces a bi-linear saw-tooth-like phase distribution as shown in Fig. 1 (c) and results in signal enhancement characteristics as shown in Fig. 2 (c). This bi-linear phase RF pulse was then applied to blood imaging of a human head. Since venous blood is believed to be deoxygenated (20), it will exhibit a susceptibility effect due to the interfaces between the surrounding tissues and the deoxyhemoglobin. In Fig. 5, an image or angiogram (venogram) obtained by the gradient echo sequence using the tailored RF pulse which produces a bi-linear phase distribution is shown. When the tailored RF pulse is applied to the gradient echo sequence, we have incorporated a gradient moment nulling which reduces the signal loss in the blood due to flow dephasing phenomena. An echo time of 20 msec was used to allow sufficient dephasing due to the susceptibility effect in the voxel. In this example of susceptibility-effect-based angiography, the transverse resolution of the image was 0.8 x 0.8 mm^2 with a slice thickness of 5 mm. Five slices were obtained contiguously, and subsequently maximum ray tracing was performed in the slice-selection direction. As is shown in Fig. 5, the image contrast is such that the signals from the normal tissues are suppressed while the signals from the regions with local field gradients due to the susceptibility effect are enhanced. This experiment demonstrates that an RF pulse can be tailored for blood imaging by using the susceptibility effect, and at the same time, it can effectively suppress the signal from the normal tissues which have no susceptibility effect.

In conclusion, a new technique for manipulating the susceptibility effect by using a series of tailored RF pulses has been proposed, and theoretical as well as experimental verifications of the method have been studied. Two examples of the method, namely, susceptibility effect compensation in the gradient echo sequence and an angiographic application based on the susceptibility effect generated by deoxygenated blood, i.e., venous blood, have been tested experimentally. Further applications of the method with a variety of tailored RF pulses for different applications are under study and will be reported later.

REFERENCES

1. K. R. Thulborn, J. C. Waterton, P. M. Matthews, and G. K. Radda, *Biochim Biochem Acta* 714, 265 (1982).

2. A. Villringer, B. R. Rosen, J. W. Bellivean, J. L. Ackerman, R. B. Lauffer, R. B. Buxton, Y. Chao, V. J. Wedeen, and J. Brady, *Magn. Reson. Med.* **6**, 164 (1988).

3. S. C. Chu, Y. Xu, J. B. Balschi, and C. S. Springer, JR, *Magn. Reson. Med.* **13**, 239 (1990).

4. S. Posse and W. P. Aue, *J. of Magn. Reson.* **88**, 473 (1990).

5. I. R. Young, S. Khenia, D. G. T. Thomas, C. H. Davis, D. G. Gadian, I. J. Cox, B. D. Ross, and G. M. Bydder, *J. of Comp. Assit. Tomog.* **11**, 2 (1987).

6. K. M. Lüdeke, P. Roschmann, and R. Tischler, *Magn. Reson. Imagn.* **3**, 329 (1985).

7. H. W. Park, Y. M. Ro, and Z. H. Cho, *Phy. Med. Biol.* **33**, 339 (1988).

8. S. Ogawa and T. Lee, *Magn. Reson. Med.* **16**, 68 (1990).

9. B. R. Rosen, J. W. Belliveau, J. M. Vevea and T. J. Brady, *Magn. Reson. Med.* **14**, 249 (1991).

10. J. C. Gore and S. Majumdar, *Magn. Reson. Med.* **14**, 242 (1990).

11. B. R. Rosen, J. W. Belliveau, B. R. Buchbinder, et al, *Magn. Reson. Med.* **19**, 285 (1991).

12. R. Turner, D. Le Bihan, C. T. W. Moonen, D. Despress, and J. Frank, *Magn. Reson. Med.* **22**, 2159 (1991).

13. Z. H. Cho and Y. M. Ro, *Magn. Reson. Med.* **23**, 193 (1992).

14. L. Pauling and C. Coryell, *Proc. Natl. Acad. Sci.* **22**, 159 (1936).

15. D. Eidelberg, G. Johnson, D. Barnes, P. S. Tofts, D. Delpy, D. Plummer, and W. I. McDonard, *Magn. Reson. Med.* **6**, 344 (1988).

16. R. A. Brooks, A. Brunetti, J. R. Alger, and G. D. Chiro, *Magn. Reson. Med.* **12**, 241 (1989).

17. K. M. Brindle, F. F. Brown, I. D. Campbell, C. Grathwohl, and P. W. Kuchel, *Biochem. J.* **180**, 37, (1979)

18. Y. M. Ro and Z. H. Cho, to be published.

19. Y. M. Ro and Z. H. Cho, accepted for publication in *Magn. Reson. Med.* (1992).

20. J. H. Jandl, "Blood: Textbook of Hematology" (Little, Brown and Company, 1987), p. 74.

FIGURE CAPTIONS

Figure 1. The various RF pulses and the respective phase distributions generated within the selected slice: (a) conventional sinc shaped RF pulse, (b) an RF pulse tailored to compensate for the susceptibility effect by forming a quadratic phase distribution, (c) an RF pulse tailored to enhance the susceptibility effect but at the same time suppress the signals from normal tissue by forming a bi-linear phase distribution. The latter pulse is believed to be suited for angiographic application.

Figure 2. Signal intensity distributions as a function of the susceptibility phase gradient, P_{sus}, when (a) a conventional sinc-shaped RF pulse is applied, (b) a tailored RF pulse producing a quadratic phase is applied, and (c) a tailored RF pulse producing a bi-linear saw-tooth-like phase distribution is applied. As is seen, for a given susceptibility-induced phase gradient, the signal intensity varies with the shape of the applied RF pulse.

Figure 3. Simulations of an imaging plane of water located 5 cm away from an air sphere with a radius of 2 cm: (a) the magnetic field map of the imaging plane, (b) the signal loss phenomenon with a conventional sinc-shaped RF pulse, (c) the reduced signal loss resulting from the application of a tailored RF pulse producing a quadratic phase distribution within a voxel, and (d) the monotonic increase in signal intensity due to susceptibility effect with iincreasing phase gradient, at least up to $\pm 4\pi/z_o$. Note also that the suppression of the signal intensity when the susceptibility effect is absent ($P_{sus}=0$). In the latter, application of a tailored RF pulse will produce a bi-linear saw-tooth-like phase distribution within a voxel.

Figure 4. (a) A human head image obtained with the conventional sinc-shaped RF pulse which produces no phase distribution within a voxel. As is seen, the signal voids around the nasal cavities are clearly visible. (b) The same image as (a) but obtained with a tailored RF pulse which produces a quadratic phase distribution. Note the complete recovery of the signals near the nasal cavities.

Figure 5. A blood imaging (venogram) of a cat head obtained with a bi-linear saw-tooth-like phase distribution within a voxel as shown in (b) while normal gradient echo imaging is shown in (a). As is seen, small vessels (venous vessels) are clearly seen due to the susceptibility effect.

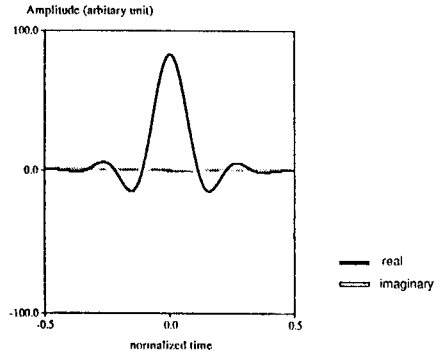

Conventional sinc shaped RF pulse

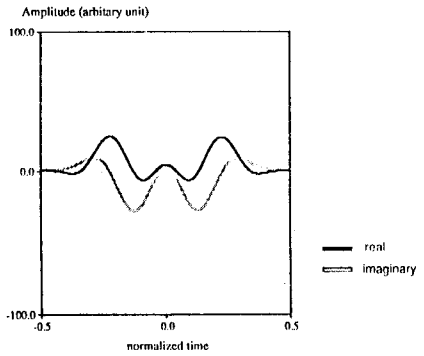

A tailored RF pulse with a bi-linear phase distribution

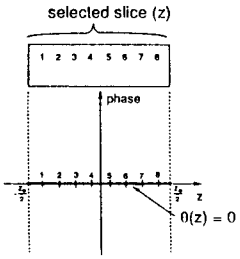

Figure 1 (a)

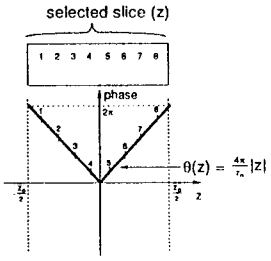

Figure 1 (c)

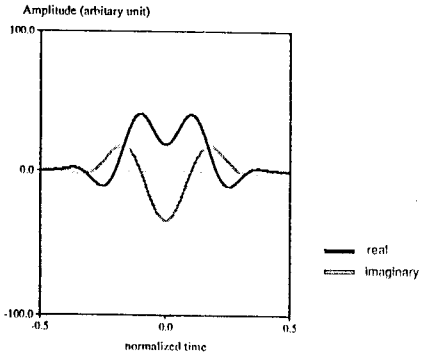

A tailored RF pulse with a quadratic phase distribution

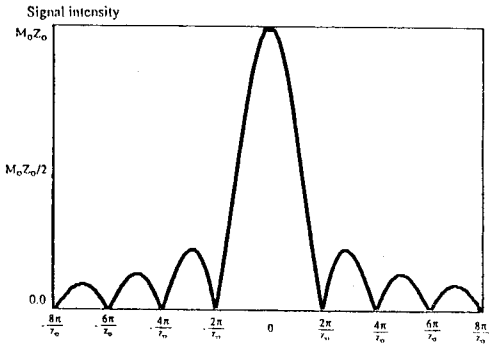

Figure 2 (a)

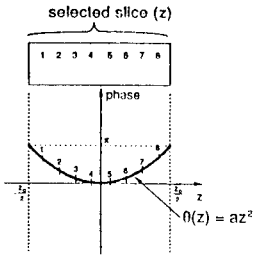

Figure 1 (b)

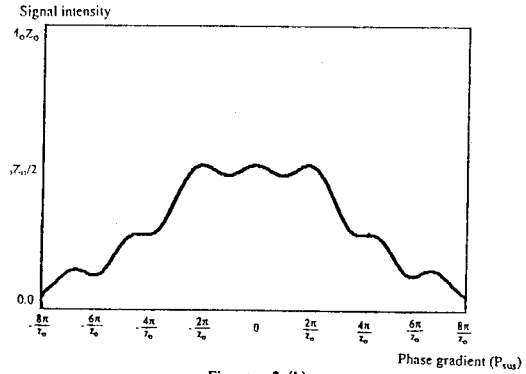

Figure 2 (b)

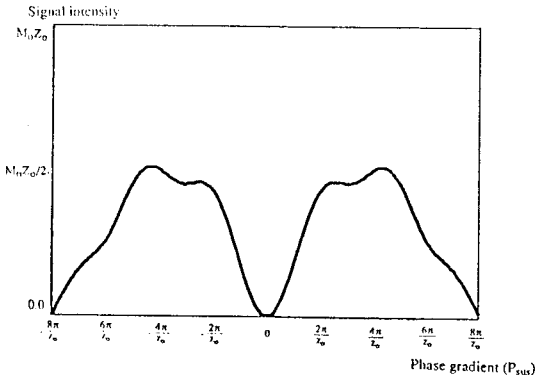

Figure 2 (c)

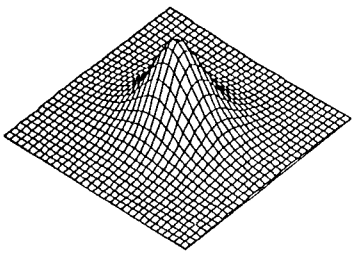

(a)

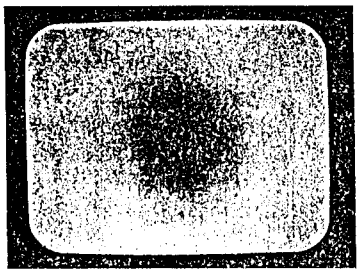

(b)

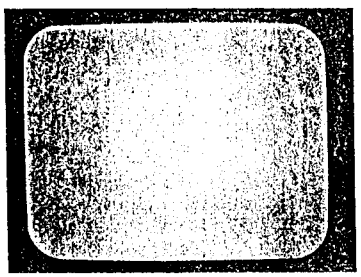

(c)

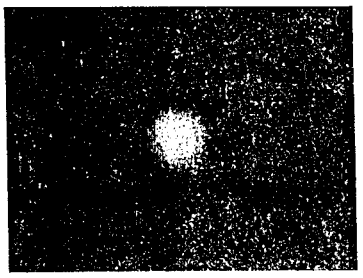

(d)

Figure 3

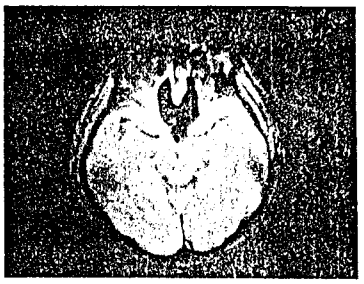

(a)

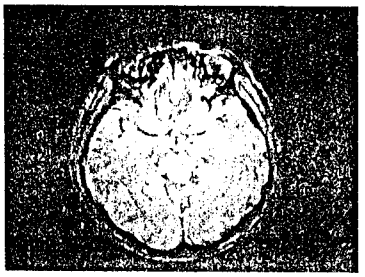

(b)

Figure 4

(a)

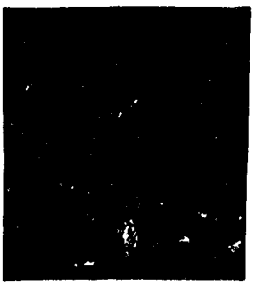

(b)

Figure 5